Structure of Heat-Treated Nylon 6 and 6.6 Fibers. II. Recrystallization Mechanism

ABIGAIL LISBÃO SIMAL, ADRIANA REGINA MARTIN

Departamento de Engenharia de Materiais, Universidade Federal de São Carlos, Via Washington Luiz, Km. 235, Caixa Postal 676, 13565-905 São Carlos, SP, Brazil

Received 17 July 1997; accepted 9 October 1997

ABSTRACT: The present work compared the recrystallization process of Nylon 6 with Nylon 6.6 fibers. For such a study, the fibers were submitted to different annealing conditions (slack and restrained conditions) in a wide range of temperatures. For the structural analysis, several techniques were applied, and among them, differential scanning calorimetry (DSC) was demonstrated to be a very important tool. Nylon 6 and 6.6 fibers responded differently to the applied annealings, indicating different recrystallization mechanisms. The Nylon 6 fiber presented the formation of new and very small crystallites in their interfibrillar regions for the annealings performed above 120°C independently of the annealing condition. In addition to their improvement in size and perfection as the annealing temperature increases, their presence favored a general recrystallization in a preferred direction, that is, of the fiber axis. The recrystallization process of the Nylon 6.6 was commanded by the disorientation process associated to the release of the hydrogen bonds. The DSC thermograms revealed two crystalline forms, that is, of the same type but with different degrees of size and perfection. At temperatures below the T_g, the less perfect crystallites are converted into more perfect ones, while at temperatures above the T_g, the intense movement of the chain segments favored a reversal in this process, that is, the more perfect ones are converted again to the less perfect form. © 1998 John Wiley & Sons, Inc. J Appl Polym Sci 68: 453–474, 1998

Key words: fibers; Nylon 6; Nylon 6.6; heat treatment; recrystallization mechanism

INTRODUCTION

Knowledge of the thermomechanical history of polymeric materials is a very important tool in the evaluation of several properties of interest, such as mechanical properties. In the case of synthetic fibers, for instance, which can be submitted to different processing conditions, the studies of the effects of different thermal annealings and processing (spinning and drawing) on their structure are of great interest and a variety of publications on this subject can be found in the literature.[1–7] Such studies can provide a better understanding of the correlation between the structure and the properties of these fibers.

Annealing is usually applied to modify the supermolecular organization of a crystalline polymer.[8] In fibers which are usually oriented, annealing may lead to a change in the structure of the amorphous and crystalline regions as well. Also, such structural changes might depend on the annealing conditions, such as the slack condition where the fibers are allowed to shrink freely, or on the restrained condition, which is more closely related to their industrial processing. The restraining of a sample to a constant length during

Correspondence to: A. L. Simal.
Contract grant sponsor: CAPES; contract grant sponsor: FAPESP.

Journal of Applied Polymer Science, Vol. 68, 453–474 (1998)
 CCC 0021-8995/98/030453-22

annealing can generate significant stresses and often affects the extent of property modification.[8] Also, the annealing temperature has a strong influence on the properties of the fibers, especially near or above their glass transition temperature.

To make a comprehensive study of the effect of these annealing conditions on the structure of the fibers, it is important to consider knowledge of the basic and more recently acceptable model for the fiber structure. It is recognized that there can be no universal or even widely applicable model of fiber structure, but it is possible to define models which are useful in the application to particular types of fibers subject to particular histories.[9]

Several structure models have been proposed over the years, leading gradually to the present fiber models that combine the results of morphological analysis with mechanical and thermal behavior, especially thermal shrinkage.[10] In the present, as a result of these studies, it is of general consensus that melt-spun fiber and drawn, such as poly(ethylene terephthalate) (PET), and nylon fibers can present at least three distinct phases: amorphous and crystalline domains of the microfibril and the interfibrillar matter.[10] This three-phase model together with the analysis of DSC thermograms has been shown to be particularly useful in explaining the shrinkage mechanism of PET[11] and Nylon 6 (refs. 5 and 12) and 6.6 (ref. 12) fibers.

An interesting aspect of the fiber structure that has been explored[5,9,11–16] to some extent is the possibility of the appearance of double melting peaks[9,12,13,15,16] and premelting peaks[5,11,12,14] in the differential scanning calorimetry (DSC) analysis of fibers submitted to different processing conditions and thermal treatments. These multiple endotherms can give us a better insight into the changes of the preexisting structural organization due to the thermomechanical treatments applied to the fibers.

Another way to overview such structural modifications in synthetic fibers due to different thermal treatments is the use of an equation of the Arrhenius type[2] to analyze several structural parameters of interest. Oriani and Simal[2] applied such an equation to several structural parameters on their studies with heat-treated Nylon 6 fibers and detected two types of behavior that depend on the analyzed parameter: The parameters' long period and shrinkage showed linearity in the temperature range of 100–190°C, while the others (lateral order, crystalline perfection index, and crystallinity percentage) presented linearity between 150 and 190°C. Also, they observed a discontinuity in the range of temperature from 100 to 150°C which was associated with the chain flexibility and responsible for the major structural rearrangement of the Nylon 6 fibers. However, this study was limited to four temperatures of heat treatment with the Nylon 6 fiber heat-treated under a slack condition only. So, the existence of such differentiated behavior when the Arrhenius equation was applied to these parameters indicated the need for more extensive work on this subject, especially in the observed discontinuity region as mentioned above.

Thus, in the present work, we intended to extend the work of Oriani and Simal[2] to Nylon 6 and Nylon 6.6 fibers for a wider range of temperatures of heat treatment and different annealing conditions, that is, with the fibers under slack and restrained conditions. We expect that this study with different nylons and different annealing conditions will allow us a better understanding of the phenomenological aspects that might be governing the different behavior as described above. In addition, we used DSC analysis to accomplish our expectations.

EXPERIMENTAL

Sample Preparation

Nylon 6 and 6.6 fibers from De Millus S/A (Rio de Janeiro, Brazil) and Rhodia S/A (Santo André, SP, Brazil), respectively, were submitted to dry heat treatments under slack and restrained conditions in an evacuated oven. The fibers were heat-treated for 2 h under an inert atmosphere at the following temperatures: 70, 80, 100, 120, 135, 150, 170, 180, and 190°C. After the heat treatments, the fibers remained in a desiccator for 30 days before data collection. The time of 2 h for the heat treatments was chosen based upon previous works by one of the present authors.[2] Also, this time of heat treatment has proved to be safe enough to avoid crystal decomposition.[17]

Although the fibers presented different origins, they possess the same level of draw ratios: 3.2× for the Nylon 6 and 3.29× for the Nylon 6.6. Also, the spinning and drawing processes for the Nylon 6 fibers were continuous, while for the Nylon 6.6, they were discontinuous.

Structural Measurements

Shrinkage

Shrinkage measurements were made by knowing the length before (S_h^0) and after (S_h^f) the heat

treatments under the slack condition. Therefore, the shrinkage percentage ($\%S_h$) was calculated through the following expression:

$$\%S_h = \frac{S_h^0 - S_h^f}{S_h^0} \times 100 \quad (1)$$

Differential Scanning Calorimetry (DSC)

DSC (from Perkin–Elmer) measurements were used to evaluate the thermograms and to calculate the crystallinities from the observed areas under the heat of fusion peaks (ΔH_f) of the samples. The crystallinity percentages ($\%C$) were calculated as follows:

$$\%C = \frac{\Delta H_f}{\Delta H_0} \times 100 \quad (2)$$

where ΔH_0 are the values of the heat of fusion for the totally crystalline Nylons 6 and 6.6 with an α phase, or 166.5 (ref. 18) and 191.0 J/g (ref. 19), respectively, and ΔH_f is the observed heat of fusion in J/g. The runnings were effectuated under an inert atmosphere at a heating rate of 10°C/min.

Dynamic Mechanical Thermal Analysis (DMTA)

DMTA (from Polymer Laboratories) runnings were used to evaluate the glass transition temperature of the samples. The running conditions were a heating rate of 3°C/min and a frequency of 10 Hz.

X-ray Analysis

Wide angle X-ray scattering was performed in a Rigaku Rotaflex diffratometer, Model R1-200B, utilizing Ni-filtered CuKα radiation. The obtained diffratograms were used to calculate the index of chain packing (ICP) and the crystal size (CS) as described in detail in the literature.[1,14,20–23]

Our Nylon 6 and 6.6 fibers presented a characteristic two-peak equatorial X-ray scattering pattern for an alpha structure as described by several authors[1,19] for all the analyzed temperatures of heat treatment. The observed peak maxima for the Nylon 6 fibers were $2\theta_1 \cong 20.3°$ and $2\theta_2 \cong 23.1°$, which correspond to the reflection planes (002) and (200), respectively, and for the Nylon 6.6 fibers, they were $2\theta_1 \cong 20.5°$ and $2\theta_2 \cong 22.9°$, corresponding to the reflection planes (100) and (010), respectively.

Murthy et al.[1] suggested a new parameter which could be calculated directly from the positions of the two intense equatorial reflections, in substitution of the crystalline perfection index (CPI) parameter.[1,20,23] The substitution is justified by the possibility of elimination of some difficulties related to the interpretation of the CPI parameter.[1,23]

Thus, this new parameter was defined[1] for Nylon 6 as the index of chain packing (ICP) [eq. (3)] and presented to be a reduced form of the CPI parameter. Also, we extended this definition for Nylon 6.6 through eq. (4) or

$$\text{ICP} = \Delta d = d\,(200) - d\,(002) \quad (3)$$

$$\text{ICP} = \Delta d = d\,(100) - d\,(010) \quad (4)$$

where Δd is the difference in angstrons of the d-spacings of the two intense equatorial peaks.

The crystal sizes (CS)[1,21] were calculated using the Scherrer equation or

$$\text{CS} = \frac{K\lambda}{\beta\,(\cos\theta)} \quad (5)$$

where K is the shape factor which varies between 0.9 and 1.1. A value of 0.90 (ref. 1) was considered for our calculations. λ is the wavelength of the radiation used (CuKα = 1.5418 Å); β, the half-maximum breath in radians; and θ, the Bragg angle.

The CS measurement corresponds to the direction perpendicular to the plane considered in the analysis.[24] For instance, the (200) and (100) reflections were used to obtain the size along the hydrogen-bonded direction, and the (002) and (010) correspond to the size along the van der Waals-bonded direction for Nylon 6[1,7] and 6.6,[25] respectively. The half-maximum breath of these reflections was obtained after deconvolution of the X-ray diffratograms. Finally, the calculated CS values should be considered as relative values only, since the necessary corrections for the Scherrer equation[21] were not made.

Small-angle X-ray scatterning (SAXS) was performed in a Statton Camera[21] fixed in a Phillips System, Model MW 1130/00/60, utilizing a rotatory anode (Ni-filtered CuKα radiation). It used a pinhole collimation with a specimen-to-film distance of 29 cm and exposure time of 24 h. The long period (LP) parameter was calculated from the meridional patterns utilizing the Bragg equation as described elsewhere.[21]

The mean thickness of the crystalline lamellae (lc) was calculated by expression (6)[15]:

$$lc = (LP) \times \%C_{DSC} \quad (6)$$

In this expression, LP stands for the mean long-period as obtained by the Bragg equation from SAXS patterns as described above and $\%C_{DSC}$ is the crystalline percentage calculated from eq. (2) by the DSC method. This equation was considered as an acceptable approximation by Groeninckx et al.[15]

Birefringence

Birefringence (Δn) was measured in a polarized light microscope (Leitz SM-LUX-POL) utilizing a Berek compensator. The same microscope was used to measure the diameter of the fibers.

RESULTS AND DISCUSSION

General Aspects

Figures 1–7 show the effects of the increasing annealing temperature on the structural parameters: crystallinity Percentage ($\%C$) measured by DSC, birefringence (Δn), crystal sizes along and perpendicular to the hydrogen bonds (CS), long period (LP), lamellar thickness (lc), and index of chain packing (ICP) for the Nylon 6 and 6.6 fibers heat-treated under different conditions (slack and retrained).

These figures reveal that Nylon 6 responds differently to the different annealings when compared to the Nylon 6.6 fibers. One of the major commanding factors for such observed differences could be their original structure before the annealings. Yet, although the fibers behave differently to the heat treatments, if analysis is made of a particular fiber (Nylon 6 or 6.6), it will be able to verify that some structural parameters are strongly interrelated, varying in unison with the different annealings (temperature and condition). As an example, we could recall the parameter shrinkage and the LP from part I (ref. 12) of this series of articles, where we were able to propose a shrinkage mechanism for the Nylon 6 and 6.6 fibers heat-treated under a slack condition.

Since the $\%C$ is a parameter that can be affected by many factors (existence or not of orientation, generation or not of new crystallites, improvement of the size and perfection of the preexisting ones), its dependence on the annealing conditions (temperature and type of heat treatment) might be influenced in a complex manner by all the analyzed parameters.

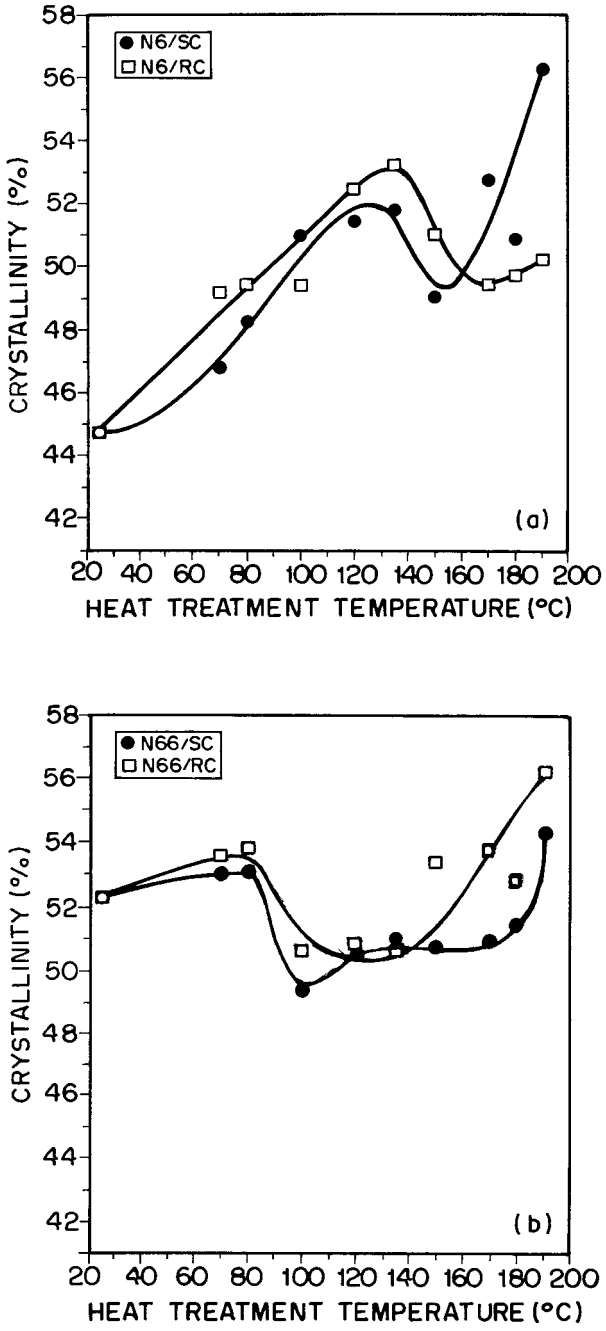

Figure 1 Crystallinity percentage vs. heat-treatment temperature for the (a) Nylon 6 and (b) Nylon 6.6 fibers heat-treated under (●) SC and (□) RC.

So, a comprehensive study of such a complex recrystallization process is necessary in order to promote a better understanding of the main phenomenological aspects envolved in the different responses to the annealings by the different fibers. Therefore, for convenience, we will present a discussion of the results for the Nylon 6 fibers

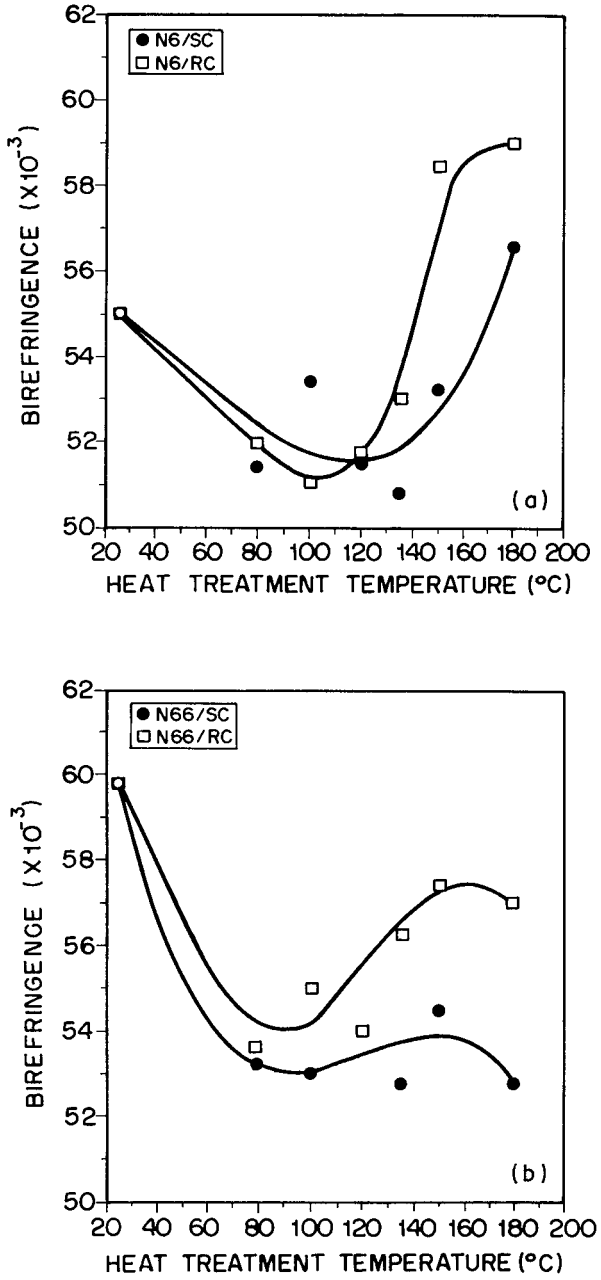

Figure 2 Birefringence vs. heat-treatment temperature for the (a) Nylon 6 and (b) Nylon 6.6 fibers heat-treated under (●) SC and (□) RC.

separately from the Nylon 6.6 ones and a comparison between these fibers will be presented in sequence.

The Nylon 6 Fiber

Figure 1(a) shows that the crystallinity parameter (*%C*) increases continuously up to the annealing temperature around 120 and 135°C for the annealing under slack and restrained conditions (SC and RC), respectively, where maxima are observed. These maxima are followed by minima around 150 and 170°C for the same annealing conditions (slack and restrained, respectively).

Also, the Nylon 6 fibers heat-treated under the

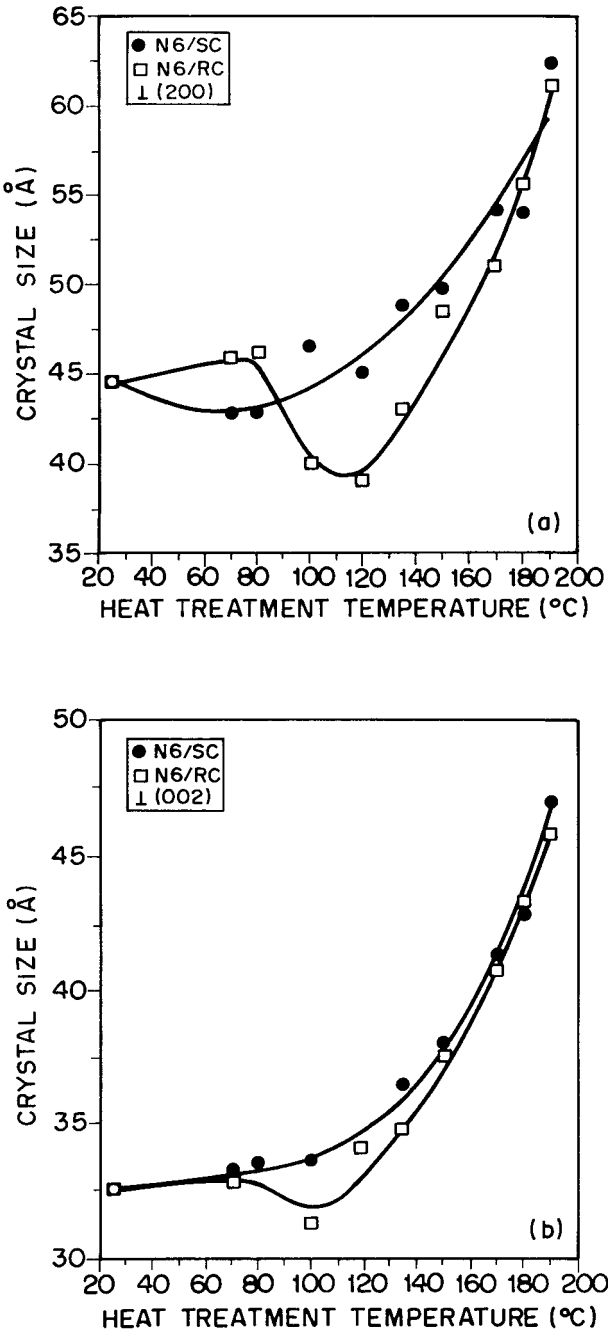

Figure 3 CS vs. heat-treatment temperature for the Nylon 6 fibers heat-treated under (●) SC and (□) RC: (a) ⊥ (200); (b) ⊥ (002).

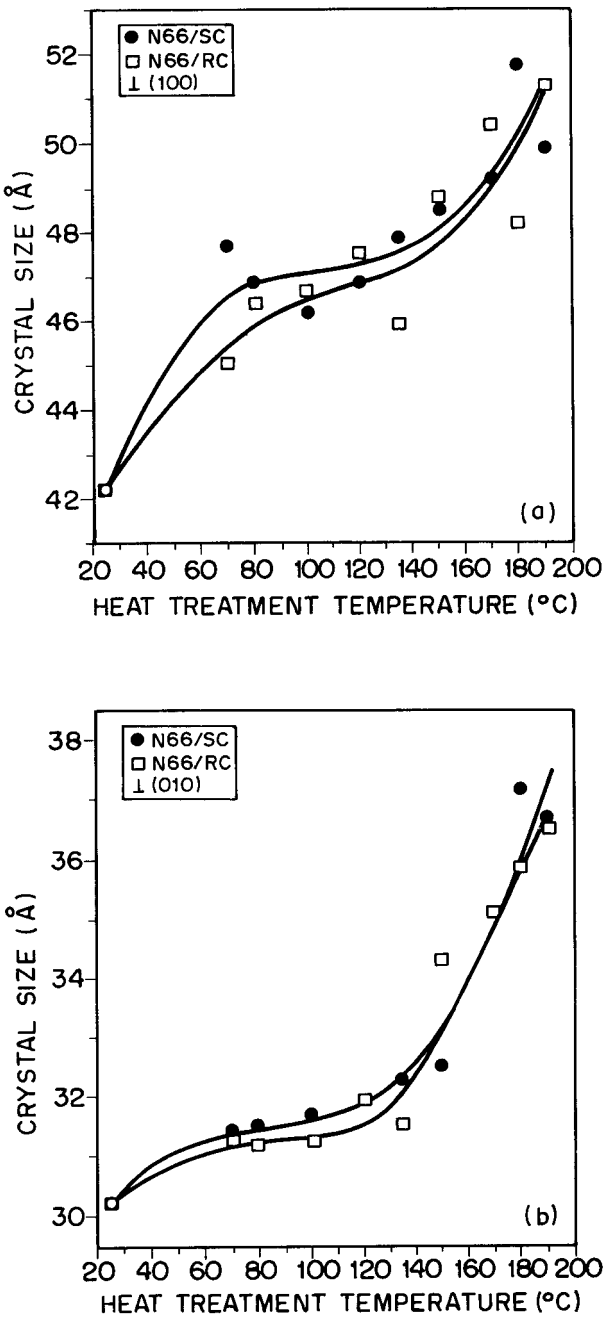

Figure 4 CS vs. heat-treatment temperature for the Nylon 6.6 fibers heat-treated under (●) SC and (□) RC: (a) ⊥ (100); (b) ⊥ (010).

RC presented higher values of *%C* for the annealing temperatures up to the observed minima points. But at higher annealing temperatures, an inversion of this behavior is evident. For the heat treatments in the range of temperatures from 150 to 190°C, Nylon 6 fibers experience a deep increase in crystallinity only when the annealings are performed under the SC, showing recovery of the partial loss of crystallinity observed in the temperatures between 120 and 150°C. For the heat treatment performed under the RC, this recovery was very small, reaching values not much higher than the minimum point at 170°C. It seems that the fiber is presenting a stabilization in its *%C* for this type of heat treatment in this range of temperatures.

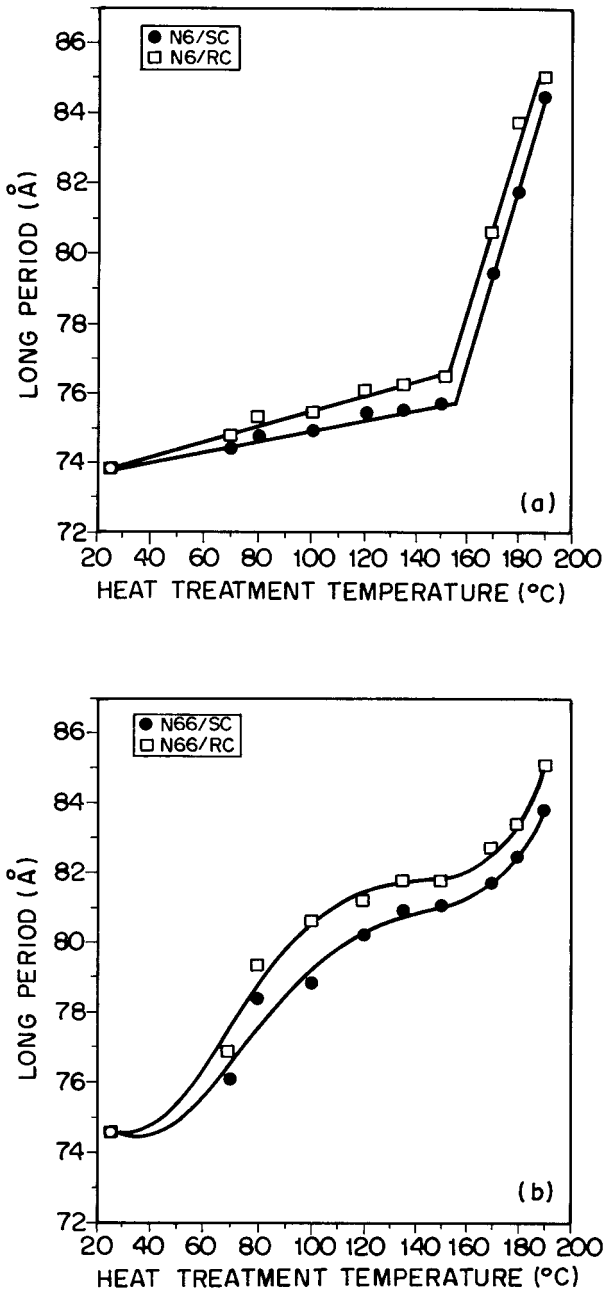

Figure 5 LP vs. heat-treatment temperature for the (a) Nylon 6 and (b) Nylon 6.6 fibers heat-treated under (●) SC and (□) RC.

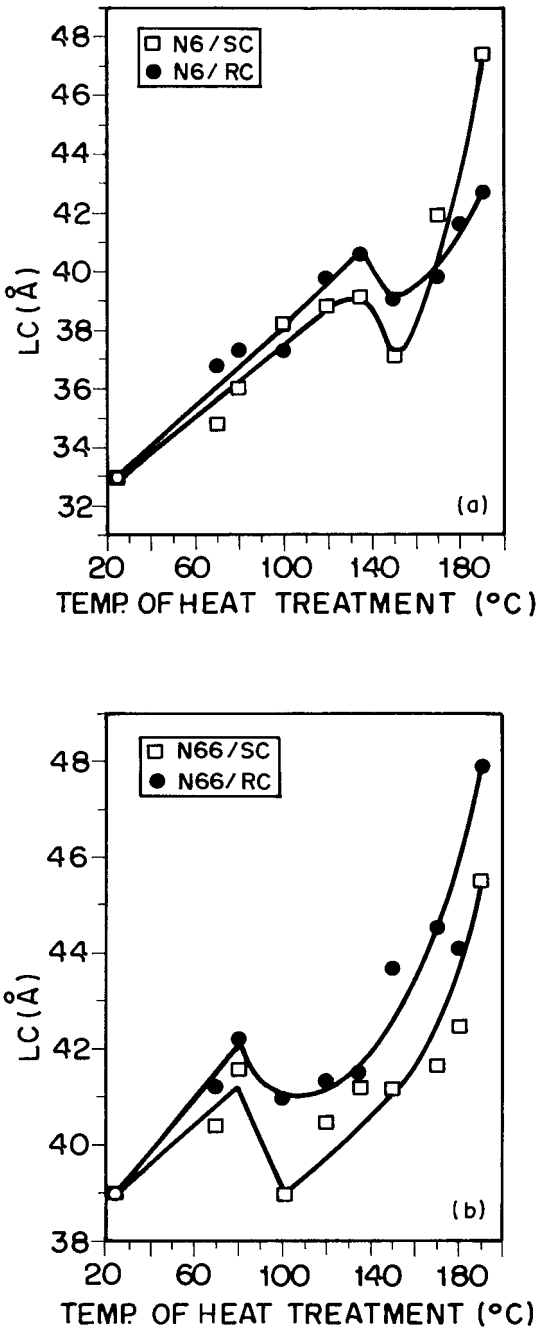

Figure 6 Lamellar thickness (lc) vs. heat-treatment temperature for the (a) Nylon 6 and (b) Nylon 6.6 fibers heat-treated under (□) SC and (●) RC.

When Nylon 6 fibers are heat-treated under the RC, one could expect that the general orientation (amorphous and crystalline regions) would be more likely to be preserved. However, this fact seems to be only partially true. Analyzing Figure 2(a), the loss in the global orientation (represented here by the Δn parameter) is clearly seen at a lower range of annealing temperatures with a minima at 100 and 120°C for the annealings under the RC and SC, respectively. But as the annealing temperature increases above the observed minima, Δn increases again and more rapidly for the annealings under RC when compared to the annealings performed under the SC.

It is well known[2] that the birefringence parameter measures the global orientation of the samples, that is, the orientation of the crystalline plus

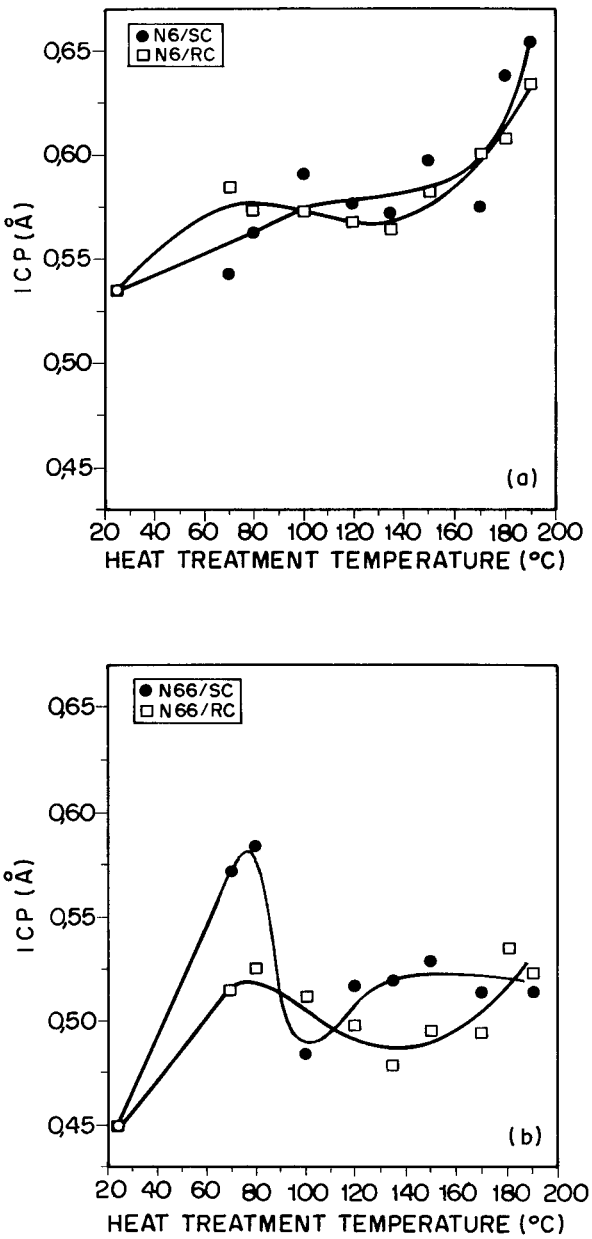

Figure 7 ICP vs. heat-treatment temperature for the (a) Nylon 6 and (b) Nylon 6.6 fibers heat-treated under (●) SC and (□) RC.

the amorphous regions. So, assuming for our Nylon 6 fibers the three-phase model as described by Prevorsek and Oswald[10] for oriented fibers, the global orientation might be reflecting the orientation of crystalline and amorphous regions within the microfibrils, as well as the orientation of the interfibrillar regions which are the noncrystalline but oriented amorphous regions. However, as the temperature increases, these regions might be responding differently to the different annealings (range of temperature and type of heat treatment) and, consequently, would affect differently the Δn value or the global orientation.

Therefore, at a lower range of temperatures (between room temperature and 100–120°C), the loss in the global orientation might be reflecting the loss of orientation mainly in the amorphous regions (mainly within the interfibrillar regions which seem to be less stable), for both conditions of heat treatments (SC and RC). This initial loss of orientation would be related to the stress relaxation due to processing (spinning and drawing). Yet, these stress relaxations are likely to be more effective when the fibers are allowed to shrink freely during the annealings (SC), since the observed crystallinities were lower for this heat-treatment condition. The length preservation during the annealings at this range of temperatures resulted in less disorientation and, consequently, higher crystallinity percentage values. Yet, this initial loss of orientation would be accompanied by the rearrangement of the preexisting crystals within the microfibrilar regions, allowing elimination of defects of the crystals, for example. This fact would have some contribution in the observed increase in the crystallinity parameter at this range of annealing temperatures (not much above its T_g of 98°C).

This suggestion seems to be confirmed by the analysis of the effect of the annealing conditions on the parameters' CS [Fig. 3(a,b)] and LP [Fig. 5(a)] in this same range of temperatures. Figure 3(a,b) shows that the CSs measured perpendicular to the fiber axis (along and perpendicular to the hydrogen bonds) do not present accentuated changes at this lower range of temperatures, especially when the heat treatment was performed under the SC. When the fibers were not allowed to shrink during the annealings, the Nylon 6 fibers experienced a decrease in the CSs measured parallel and perpendicular to the hydrogen bonds, with minima around 100–120°C (near its T_g of 98°C), which could be the temperatures necessary to release their hydrogen bonds. This effect was more pronounced for the CS measured along the hydrogen bonds. These minima seem to reflect the conformational changes imparted by the loosening of such bonds as a consequence of the mobility of the chains for the annealings performed at temperatures near the T_g. The annealings under the RC did not avoid such conformational changes, but made difficult the thickening of the crystals, resulting in smaller CSs when compared to the heat treatment under the SC for the annealings performed at temperatures above the T_g of this fiber.

In addition, to have significant crystal growth at the direction perpendicular to the fiber axis, the release of N—H and C═O bonds are of fundamental importance. In fact, the effective crystal growth was observed only for the annealings performed above 120°C for both types of heat treatments (SC and RC).

Therefore, the disorientation process due to stress relaxation at the lower range of temperatures might be contributing more to an increase in the lamellar spacing in the direction to the fiber axis as revealed by Figure 5(a) than to the crystal growth measured as described above. As can be seen in Figure 5(a), the LP parameter presented a small but continuous increase up to the heat-treatment temperature of 150°C. A deep increase in this parameter is observed only for the heat treatment above this temperature.

The observed increase in the lamellar spacing can be used to calculate the mean thickness of the crystalline lamellae (lc) using eq. (6). The approximations and the physical significance envolved in the utilization of this equation can be found in the literature[15] and will not be discussed here. The utilization of eq. (6) resulted in Figure 6(a), which demonstrates that the lamellar thickness parameter follows the same curve pattern as described by the crystallinity parameter, increasing continuously in the range of temperature from 25 to 135°C with a partial decrease at the heat-treatment temperature of 150°C. So, the increase in the LP parameter at this temperature did not compensate for the loss of crystallinity as already described. Some compensation occurs only at high annealing temperatures (above 150°C) where a deep increase in the LP was observed.

These results confirm the earlier suggestion that the observed increase in the crystallinity parameter at the lower range of annealing temperatures occurs mainly by defect elimination of the preexisting crystals which would result in the increase of the lc in the direction parallel to the

fiber axis. This increase in the lc would result in a decrease in the interlamellar spacing. Indeed, by subtracting the lc from the LP parameter, we can visualize a slight reduction in the interlamellar distance from 41 to 37 or 36 Å for the annealings at the lower range of temperatures (from 25 to 135°C) for both annealing conditions. Above 135°C, the interlamellar distance increases again, returning to their original values prior the annealing, about 40–42 Å. This behavior can be better understood in the following discussion.

All the major structural transformations occur only for the heat treatments above the T_g of this fiber. The increase of chain flexibility will deeply affect the recrystallization process.

As mentioned before, in spite of the sharp increase in the crystalline sizes along the hydrogen and van der Waals bonds for the annealings above 120°C ($\sim$ 20°C above the T_g), this fiber is experiencing a partial loss in the crystallinity parameter in the range of temperatures from 120 or 135 to 150 or 160°C depend on the annealing condition. This observed loss of crystallinity might be related to an additional loss of orientation of the amorphous regions due to the intense chain flexibility in this range of temperatures. This additional loss of orientation in this range of temperatures might occur not only in the interfibrilar regions, but also in the interlamellar regions as well. As mentioned before, the Δn parameter presented a minimum at an annealing temperature around 120°C. The observed increase in the global orientation above this temperature might be a result of a subsequent recrystallization in the direction of the fiber axis. The length preservation of the fibers during the annealings above 120°C will result in higher Δn values when compared to the annealings where the fibers were allowed to shrink freely.

DSC Analysis for the Nylon 6 Fiber

As mentioned in part I of this series of articles, the DSC thermograms of the Nylon 6 fibers revealed a premelting peak for the annealings above 120°C, when the fibers were heat-treated under the SC. Now, analyzing the DSC thermograms of these fibers heat-treated under the RC, we can observe the same type of premeltings as can be seen in Figure 8. Also, the temperature of occurrence of these premeltings increases linearly with the annealing temperature. The only difference observed between the two annealing conditions is that under the RC the premeltings occur at lower temperatures for the annealings carried out above 170°C. This fact might be the consequence of the formation of less perfect crystallites when the annealings are performed under the RC.

So, the recrystallization process occurs similarly for both types of annealings for all analyzed temperatures, presenting only the small differences as already discussed. These premelting peaks have been related in the literature[1,5,12,14] to the appearance of very small crystallites in the interfibrillar regions composed by extended, but noncrystalline chains. The appearance of the premeltings in both types of annealings demonstrated that the annealings at a constant length do not prevent the relaxation in the interfibrillar extended and amorphous chain molecules, which allows the formation of these tiny crystallites within these regions. This fact means that the driving force necessary to change the conformations of the extended interfibrillar chains to a more randomly oriented one will depend on other factors, such as the loosening of the hydrogen bonds and the extent of orientation of such molecules. This is a very interesting behavior since this would be a morphology more closely related to the morphology obtained in the spinning line.

So, in this middle range of annealing temperatures, between 135 and 150–160°C, the additional loss of orientation in the interfibrillar regions would be responsible for the generation of new and very small crystallites. But these new crystallites did not increase the global $\%C$. The contribution of these new crystallites in the total $\%C$ was, on average, about 1–1.5% only, as calculated from the area of the premelting peaks from the DSC thermograms. In fact, as mentioned before, that the global crystallinity decreases at this range of temperatures reinforced the suggestion of the loss of orientation in the interlamellar regions as well. This loss of orientation in the interlamellar regions might be affecting the crystalline orientation and, consequently, the global orientation as detected by the Δn parameter. These events are coincident with the release of hydrogen bonds which occur for the annealings above the T_g of the fibers (around 120°C). It has been mentioned in the literature[1] that the fraction of free N—H groups can increase considerably at a well-defined temperature. The increased lifetime of the free N—H group might enhance the longitudinal mobility of the molecules,[1] resulting in loss in the global orientation.

Murthy et al.[1] suggested in their studies with Nylon 6 fibers that in addition to the formation

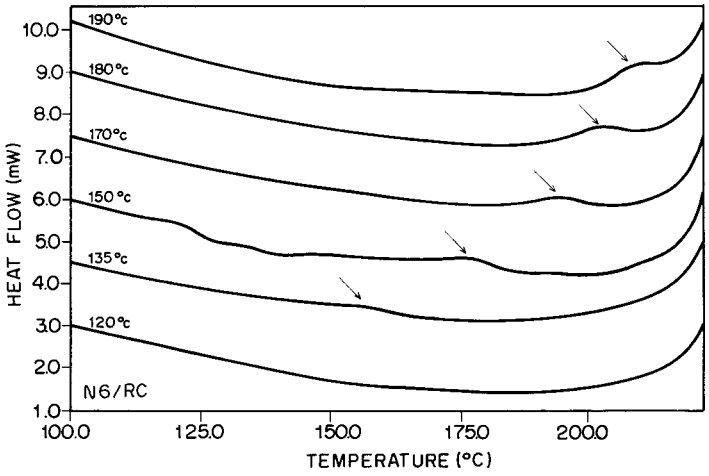

Figure 8 DSC thermograms for the Nylon 6 fibers heat-treated under RC at several annealing temperatures. The arrows indicate the premelting peaks.

crystallites in the interfibrillar regions the longitudinal movement of the chains can promote the tilting and shifting of stacks of crystalline lamellae which were initially constrained within a microfibril. This fact would contribute to their observed loss of crystalline orientation at annealings above 170°C at a dry condition.

In our case, the observed decrease in the lc values for the annealings between 135 and 150°C might be reflecting this loss of orientation, probably due to a similar mechanism as described by Murthy et al.[1] Since the LP increases slightly but continuously up to the annealing temperature of 150°C, the lc value calculated by eq. (6) reflects strongly in this range of temperatures the decrease in the global crystallinity, which, in turn, is strongly influenced by the loss of orientation. Besides the loss of orientation, the enhanced chain mobility might be promoting surface reorganization of the lamellae, such as surface melting[1] that would have some contribution to the lc value and in the loss of global crystallinity. It is clear that this loss of crystallinity is not being compensated by the new crystallite formation in this range of temperatures. Also, as mentioned before, it is at the annealing temperature of 135°C that the interlamellar amorphous regions start to increase again and that might be the contributing factor for this increase in the LP parameter. An increase in the lamellar spacing might contribute to the thickening of the crystalline lamellar regions as well as of the interlamellar amorphous regions.

As the annealing temperature increases, the chain mobility is intensified, allowing coalescence of the new crystallites within the interfibrillar region, improving their size and perfection. The dislocation of the premelting peaks to higher temperatures substantiate this fact. Also, similar changes in the microfibrillar regions (crystalline lamellae and interlamellar amorphous regions) will occur.

Segregation of kinks or other defects from within the crystalline lamellae into the interlamellar regions[1] might also be favored by longitudinal translation (self-diffusion of the macromolecules). All these structural changes will result in the observed increase not only in the CS measured perpendicular to the fiber axis but also in the lc value measured along the fiber axis.

From our observed data, we could also suggest that with the improvement of the size and perfection of the new crystallites within the interfibrillar regions (coalescent crystallites) additional loss in the global orientation will be difficult. Actually, the recrystallization process will occur in the preferred direction, that is, the direction of the fiber axis as supported by the increase in the Δn parameter.

The smaller $\%C$'s observed for the annealings under the RC above 160°C might be related to smaller and less perfect crystals measured perpendicular to the fiber axis and in the direction along the hydrogen bonds as explained before in the text. In addition to the movement restriction imposed by the presence of the new crystallites in the interfribillar regions, the longitudinal translation of the molecules will be difficulted for the annealings under the RC.

The prior discussion suggests for this Nylon 6

fiber three well-defined regions for the recrystallization process, which are clearly visualized in Figure 1, where the crystallinity parameter measured by DSC was analyzed as a function of the annealing temperature: one for the heat treatments below its T_g, a second one between 100 and 150°C or 100 and 160°C depending on the type of heat treatment (SC or RC, respectively, which would include the maxima points), and the third one for the annealings at high temperatures (above 150 or 160°C).

In an independent experiment by X-ray scattering, the ICP parameter shows good agreement concerning the three regions mentioned above [see Fig. 7(a)]. At temperatures of heat treatment below the T_g, the ICP increases, slowly, presenting a plateaulike region between the range of temperatures of 100–150°C and a deep increase only for the heat treatments above 150°C. This ICP behavior seems to be independent of the heat-treatment condition (SC or RC). All the phenomenological aspects already described will fit the ICP curve format.

Murthy et al.[1] demonstrated for their Nylon 6 fibers that an increase in the ICP would imply stronger van der Waals interactions (smaller distance between hydrogen-bonded sheets) and a larger separation of the hydrogen-bonded chains. Changes in the conformation of the amide and carboxyl groups might permit the closer packing of the hydrogen-bonded sheets. They also observed pronounced changes in the structure and morphology above 170°C, which is coincident with the temperature of the maximum crystallization rate of Nylon 6. Our data suggest that these major transformations would occur at temperatures above 150°C or at lower temperature where the crystallization rate is maximum for Nylon 6.

Nylon 6.6 Fiber

Figure 1(b) shows a different format for the curve of $\%C$ as a function of the annealing temperature for the Nylon 6.6 fiber when compared to the one obtained for Nylon 6. This fact suggests that the recrystallization process of Nylon 6.6 follows a different mechanism.

This figure reveals that when the Nylon 6.6 fiber is annealed under the SC the crystallinity parameter (measured by DSC) increases slightly until the annealing temperature of 80°C; then, it presents an accentuated decrease with a minimum at 100°C, followed by a plateaulike region (with slight recovery in the crystallity) between 120 and 170°C, increasing again only for the annealings above 170°C. When the annealings are performed under the RC, the fiber also presents a deep decrease in the crystallinity parameter, with a plateau from 100 to 135°C (or a wide minimum region), increasing again when heat-treated above 135°C. The major differences observed between the two types of heat treatments are related to the extent of the plateau region and the amount of recovery in the $\%C$ at higher annealing temperatures. When the Nylon 6.6 fiber is not allowed to shrink during the heat treatments, the extent of the plateau region is shorter and the $\%C$ reaches higher values at higher temperatures of heat treatments. Also, the $\%C$ reached at 190°C was not much higher than the $\%C$ reached at 80°C, especially for the annealings where the fibers were allowed to shrink freely.

Therefore, similarly to the Nylon 6 fiber, we can define three regions of behavior for the crystallinity parameter: one at temperatures below the T_g (from 25 to 80°C), a second one in the range of temperatures above 80–135 or 150°C (depending on the annealing condition), and, finally, a third one above these temperatures (135 or 150°C).

Although the three regions of behavior occur in almost the same range of temperatures for the Nylon 6 fiber, the curves are different in format, indicating a different mechanism of recrystallization for Nylon 6.6 when compared to Nylon 6, as mentioned before.

The partial loss in the crystallinity parameter occurs earlier for the Nylon 6.6 fiber, that is, for annealings near the T_g ($\sim$ 115°C), and contrarily to Nylon 6, its loss of crystallinity is much deeper, reaching lower values than its original crystallinity, that is, prior to the annealings.

Yet, as detected for the Nylon 6 case, the ICP parameters are in good agreement with the crystallinity results [see Fig. 7(b)] for both types of heat treatments. As can be seen in this figure, there is a very good resemblance in the format of the curves. This fact is relevant since these parameters ($\%C$ and ICP) were measured by independent techniques: DSC and X-ray scattering, respectively. When the Nylon 6.6 fibers are heat-treated under the SC, the ICP increases for the annealings between room temperature and 80°C, then decreases deeply at annealing temperatures around 100°C, which is near the T_g of fiber ($\sim$ 115°C), and recovers somewhat followed by a plateaulike region for the annealings above 120°C.

Therefore, the loss of crystallinity for the an-

nealings in the T_g region reflects the loss of chain packing as a consequense of the loosening of the hydrogen bonds. The conformational changes at this transition region are playing a very important role in the recrystallization mechanism of the Nylon 6.6 fiber.

At a lower range of temperatures (25–80°C), the slight increase in the crystallinity parameter reflects mostly the defect elimination within the preexisting crystals. These defect eliminations are accompanied by a disorientation process, as detected by the birefringence data [Fig. 2(b)], where minima are observed at temperatures around 80°C for both types of heat treatments.

As we explained before, the Δn parameter reflects the global orientation of the sample (amorphous plus crystalline regions). Similarly to the Nylon 6 fiber if we consider the same three-phase model[10] to describe the morphology of our Nylon 6.6 fiber, this global orientation would reflect the orientation in the microfibrillar region and interfibrillar region as well.

The observed decrease in the Δn at this lower range of temperatures might reflect mostly the disorientation in the interfibrillar region which is more instable. Again, this instability would be the result of the presence of residual stresses in the fibers due processing (spinning and drawing). As the temperature of heat treatment is increased to 80°C, some stress relaxation will take place. Above this temperature, Figure 2(b) reveals another important result concerning the type of heat treatment applied to the fibers. When the annealings are performed under the SC, the Δn parameter presents a stabilization in its values, while under a the RC, the Δn values increased accentuately. Yet, as expected, the Δn values are higher for the annealings performed under the RC for all analyzed temperatures. But differently from the Nylon 6 fiber, the recovery in the Δn value, as the annealing temperature increases, did not supplant the Δn value prior to the annealings. So, the length preservation during the annealings did not avoid additional disorientation of the fiber structure.

Therefore, it seems that the recrystallization process of the Nylon 6.6 fibers heat-treated under the SC occurs with no preferred orientation as observed for Nylon 6.

In this annealing condition, the changes in the conformation of the chains imparted by the release of hydrogen bonds at temperatures near and above the T_g might disorient not only the amorphous regions, but also the crystalline regions. The first part of these of articles[12] already suggested such a disorientation process associated with the proposed shrinkage mechanism for this fiber.

Figure 4(a,b) shows the influence of the annealing temperature and condition in the crystal sizes of the Nylon 6.6 fibers measured in the direction along and perpendicular to the planes of the hydrogen bonds, respectively. As can be seen, the crystal sizes measured in both directions behave similarly for the different annealing conditions (RC and SC), that is, the format of the curves are pretty much the same. Also, different from the Nylon 6 fibers, the calculated values did not differ much from one annealing condition to the other. At the lower range of temperatures, the CS seems to be only slightly smaller for the annealings performed under the RC.

Another interesting observation is that the CS measured along the van der Waals bonds will effectively present a deep increase only for the annealings above 135°C, while the CS measured along the hydrogen bonds presents already a more accentuated and instantaneous increase for the heat treatment of 80°C, followed by some stabilization for the annealings between 80 and 135°C and a deep increase above 135°C.

Now, if we compare the behavior of the curves of the LP parameter [Fig. 5(b)] with the curves of the CS measured along the hydrogen bonds, a very good resemblance in the format of the curves is again detected.

The LP parameter measures the average distance of the lamellar spacing along the fiber axis, and as already discussed in the first part of this series of articles,[12] it is strongly related to the shrinkage of the fiber. However, our data revealed that the LP responds similarly to the different types of annealings (RC and SC), being only somewhat higher for the annealings performed under an RC. So, the length preservation of the fibers during the annealings did avoid the rearrangement of the crystals with increase of the annealing temperature in all directions, that is, along and perpendicular to the fiber axis.

The similarity in the format of the curves of the LP and the CS along the hydrogen bonds indicates the strong dependence of these parameters to the release of hydrogen bonds. The thickening of crystals along and perpendicular (but along to the hydrogen bonds) to the fiber axis occur simultaneously. The growth of crystals along the van der Waals directions will take place effectively only after some conformational accommodation of

the chains along the hydrogen bonds at annealing temperatures around 135°C. Above this temperature, while the CS along the hydrogen bonds increases only an additional ~ 4% at the annealing temperature of 190°C, the CS along the van der Waals bonds increases about 14%, indicating that much of the total crystal growth along the hydrogen bond has already taken place at the temperature of heat treatment of 135°C and this growth is accompanied by a simultaneous thickening of the lamellar spacing along the fiber axis.

So, all the crystallinity loss observed in the range of temperatures of heat treatment from 80 to 135 or 150°C (depending on the annealing condition) are due to loss in the global orientation (amorphous plus crystalline regions) as mentioned earlier in this article. The crystal growth observed at this range of temperature did not affect the total crystallinity percentage. At this range of temperature, this fiber is experiencing only rearrangement of the existing crystals due to an intense chain flexibility, with no additional gain in the crystallinity percentage.

Actually, the intense chain flexibility of the chains at this range of the temperature seems to be responsible for the observed loss in the global orientation. The initial loss of orientation (below the T_g) due to stress relaxation, which initially occurs mainly in the interfibrillar regions, is followed by additional disorientation not only in the interfibrillar regions, but also in the microfibrillar regions, which consist of a sequence of lamellar crystallites and interlamellar amorphous chains. The intense movement of the chains due to the disruption of the hydrogen bonds in the amorphous regions (interlamellar and interfibrillar) interfer in the initial orientation of the crystallities, promoting a more random position of the crystallites. This phenomenon is favored especially when the annealing is realized with fibers in the slack condition, which presented a wider plateau region in the curves of crystallinity percentage versus annealing temperature [Fig. 1(b)].

At higher temperatures of heat treatment (above 135 or 150°C), the recovery in the crystallinity percentages occurs in two different ways depending on the type of heat treatment:

- When the fibers are allowed to shrink freely during the annealings, this recovery will be by growth and perfection of the preexisting crystals, not only in the direction along the fiber axis, but also in the perpendicular direction, mostly now along the van der Waals bonds and with no preferred orientation.
- When the fibers are not allowed to shrink freely, all the above-described recrystallization processes occur but the additional gain in the $\%C$ observed in Figure 1(b), will be favored by some preservation in the global orientation as detected by the Δn results. So, the recrystallization (improvement of the size and perfection) occurs with some preservation orientation along the fiber axis.

To better understand the phenomenological aspects associated with the recrystallization process just described for the Nylon 6.6 fiber, we will be presenting in the sequence the results of our DSC data for this fiber.

DSC Analysis for the Nylon 6.6 Fiber

As already presented in the first part of these series of articles,[12] this fiber did not present any sign of premelting formation in the DSC thermograms as observed in the case of the Nylon 6 fibers. Actually, the Nylon 6.6 fibers presented only the formation of two main melting peaks for all annealing conditions and temperatures. This result can be clearly seen in Figure 9. Also, Figure 9 shows that the double melting peak occurs even for the non-heat-treated fibers (controls). It has been suggested in the literature[9,13,15,16] that such double melting peaks would be representative of the existence of two different crystallite forms in the fibers.

Hearle[9] presented a very good discussion on the thermodynamic and structural interpretation of the differences between the two crystallite forms suggested earlier by Sweet and Bell.[13] Although there is some controversy concerning the appearance of such a double melting peak in DSC experiments,[9,26] the existence of these characteristic peaks in the DSC thermograms of our Nylon 6.6 fibers (before and after the annealings) is a strong indication of the existence of a crystalline region with two types of crystallite forms that could be different crystallite morphologies or crystallites of the same type but with different sizes and perfection. Also, the arguments presented by Hearle[9] would confirm such a suggestion. Our fiber, after the annealings, would present a very stable structure to be influenced by the DSC running condition, such as the rate of heating.[9]

So, considering the existence of two crystalline forms for our control Nylon 6.6 fibers, the DSC

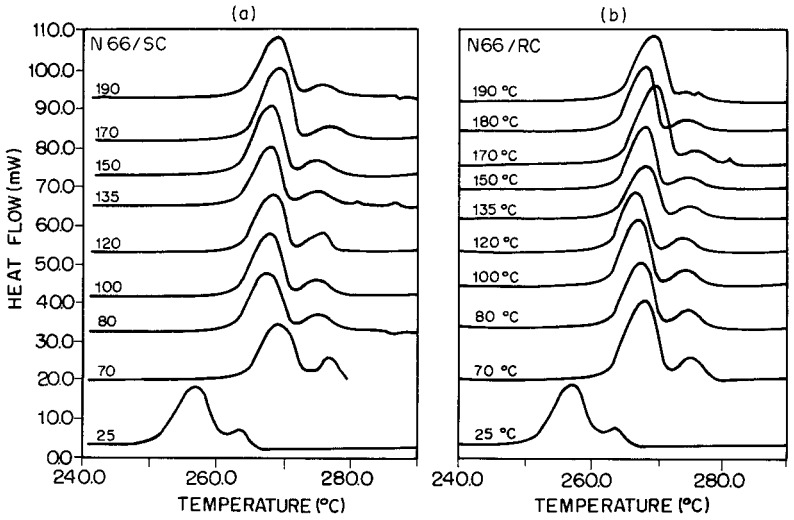

Figure 9 DSC thermograms for the Nylon 6.6 fibers heat-treated under (a) SC and (b) RC at several annealing temperatures.

thermograms (Fig. 9) reveal a dislocation of such melting peaks to higher temperatures for all annealing conditions and temperatures. So, the annealings of the fibers resulted in an increase of the melting temperatures of the crystallites and such an increase would be representative of the improvement of their size and or perfection.[9]

The double melting peaks before the annealings occur at temperatures around 257°C (peak 1) and 263°C (peak 2), and after the annealings, they appeared at temperatures around 268 and 276°C, respectively. These melting temperatures remained constant for all annealing conditions (type and temperature). The constancy of the melting temperatures of the observed peaks suggests that they are a well-defined state.[9] The major differences concerning these observed peaks were that their area would be proportional to the amount of such different crystallites in the structure of the fiber. For all analyzed conditions, the area of peak 1 was much bigger than the area of peak 2. Therefore, we could affirm that the crystalline regions of this fiber might be formed of a large amount of smaller and less perfect crystallites plus a smaller amount of bigger and more perfect ones.

The simultaneous dislocation of the peaks to higher temperatures after the annealings suggest that these crystallite forms would be of the same type although with different degrees of size and perfection.[9] The two melting peaks become much more defined after the annealings, with no overlapping as detected in the case of control fibers (prior to the annealings).

The calculation of the melting peak areas permitted the knowledge of the exact proportion (in percentage of the total area) of each crystallite form in the crystalline structure of this fiber and also the interpretation of the effect of the annealing conditions on the crystalline structure. Therefore, Figure 10 shows that as the area percentage

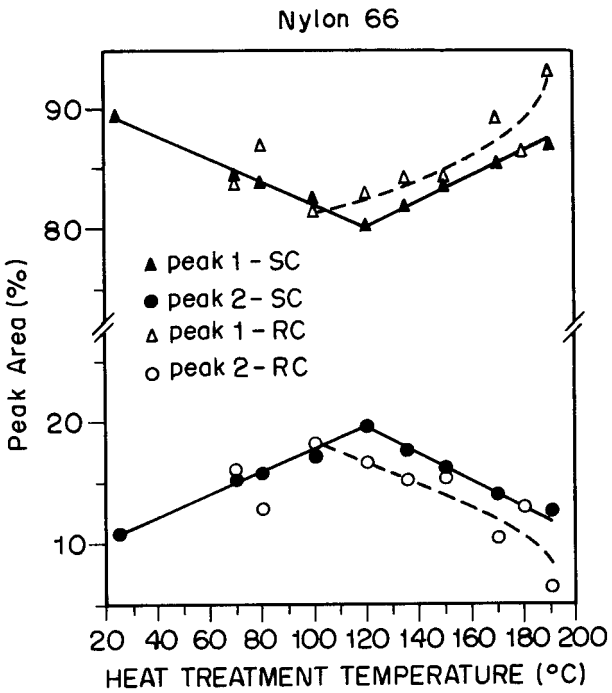

Figure 10 Peak area percentages vs. heat-treatment temperature for the Nylon 6.6 fibers heat-treated under (▲, ●) SC and (△, ○) RC.

of peak 1 decreases up to the annealing temperatures of 100 and 120°C (depending on the annealing condition), the area percentage of peak 2 increases simultaneously up to the same temperature. After this temperature, while the area of peak 1 increases again, the area of peak 2 decreases. This behavior is being followed by two types of heat treatments (SC and RC). The major differences between the two types of heat treatments are that under the RC the change in the behavior of the peaks occurs earlier (at 100°C) than under the SC (at 120°C). Also, above this temperature, the area of peak 1 seems to be somewhat bigger when the annealings are performed under the RC and the opposite is observed when we analyze the area of peak 2.

Also, it is interesting to note that under the SC the two sections of the curves (corresponding to the two ranges of temperatures) are much more linear. This linearity might be related to the easy crystallite reorganization when the fibers are allowed to shrink freely. It is clear that at this condition the crystals would be more perfect. This observation would explain also the fact the area of peak 1 is bigger for the annealings performed under the RC at higher temperatures. As we mentioned before, peak 1 would correspond to the fusion of less perfect crystallites and their amount would be higher for the annealings performed under the RC.

Finally, the changes in the proportions of the peak areas as the annealing temperature increases suggest the following mechanism:

- At the lower range of temperatures (below the T_g of the fiber), the defect elimination associated with the global disorientation process (mainly in the interfibrillar regions due to release of residual stresses), as already explained, favors the increase in the proportion of bigger and more perfect crystallites (represented by the area of peak 2). It seems that the decrease in the proportion of the less perfect crystallites might be a consequence of their partial transformation to more perfect ones.

  The accentuated increase observed in the crystal size along the hydrogen bonds at temperatures near the T_g of this fiber seems to confirm the growth of such crystals by defect elimination as the disruption of the hydrogen bonds increases with increase of the annealing temperature.

  By comparing Figures 5(b), 6(b), and 11, one could come to the conclusion that most of the observed increase in the LP parameter at temperatures around the T_g of this fiber is due mainly to an increase in the interlamellar regions (Fig. 11). Besides the thickening of the lamellar regions, the dimensions of the interlamellar amorphous regions might increase and thus contribute to the increase in the lamellar spacing.[1] Again, the intense chain flexibility imparted by the increase of the free N—H groups at this range of temperatures might contribute to such a process. Also, it is possible that the thinner or less perfect lamellae (as represented here by peak 1) might experience more easily some surface premelting that would result primarily in an increase in the interlamellar spacing and, second, to their transformation into more perfect crystallites.
- At temperatures above the T_g, the area of peak 2 decreases proportionally. This result indicates a reversal behavior with increase of the annealing temperature, that is, as the temperature increases, the more perfect crystallites are converted to their more disorganized form. Hearle[9] described a very good thermodynamic argument for such a possibility.

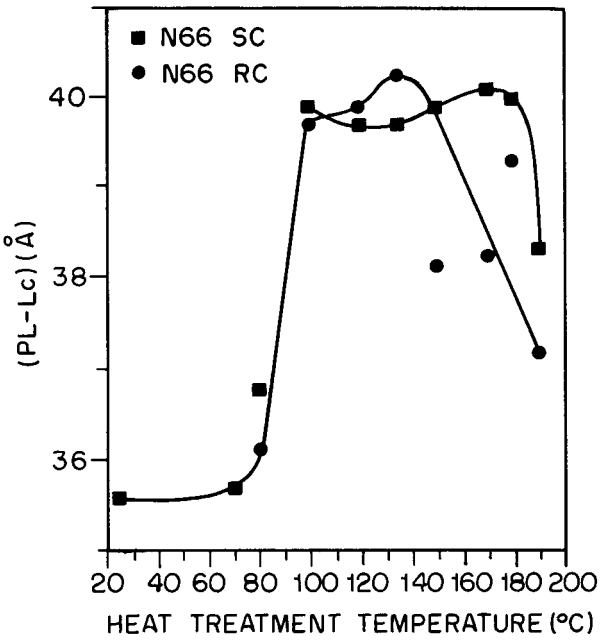

Figure 11 Interlamellar thickness vs. heat-treatment temperature for the Nylon 6.6 fibers heat-treated under (■) SC and (●) RC.

The basic crystalline structure of our Nylon 6.6

fiber is constituted by a larger amount of smaller or less perfect crystallites, which appear in our DSC thermogram as peak 1. Above the T_g, the intense movement of the chain segments would break up the more perfect alignment of the chain segments which form the crystallites correspondent to peak 2, establishing, therefore, a more uniform distribution of the segments, although less organized. This would be a stable form with increase in the internal energy compensated by increase in the entropy.[9] This fact together with the earlier suggestion that the two peaks represent the fusion of crystallites of the same type, but with different sizes or degrees of perfection, might indicate that the more perfect crystallites would be located in the immediate vicinity of the amorphous regions that is, mainly in the vicinity of the interfibrillar regions.

As can be seen in Figure 5(b), the long spacing parameter presents a plateaulike region in the range of temperatures from 100 to 150°C. At the same range of temperatures, the lc presented a decrease [Fig. 6(b)], while the interlamellar amorphous region remains practically constant (Fig. 11). These results indicate that in this range of temperatures the disorientation process associated with the release of hydrogen bonds is the principal phenomenon that will occur in the structure of this fiber with no additional increase of $\%C$, which will be occur only above 150°C where an accentuated increase in the CS along the van der Waal bonds and LP can be observed. Above this temperature, the LP will increase mainly due to increase in the crystalline lamellae. The chain segments would present an intense longitudinal movement (along the chain axis) capable of promoting additional disorientation in the interlamellar regions and in the crystalline regions as well. As a consequence of this process, the more perfect crystallites located in the vicinity of the amorphous regions will suffer a continuous disruption of their chain segments, transforming such crystallites into less perfect ones. Unlike Nylon 6, the Nylon 6.6 fibers will not have any restriction on the longitudinal movement of their chains.

Application of the Arrhenius Equation to the Structural Analysis

As discussed in the previous section, the recrystallization mechanism of Nylon 6 is different from that of the Nylon 6.6 fibers. So, to better understand the thermal effects on the structure of these fibers through the changes on the analyzed parameters, the activation energies were determined using the Arrhenius equation,[2] $\ln K = (\Delta E)/(RT) + \text{constant}$, where K is related to the parameter to be studied, T is the absolute temperature, R is the universal gas constant, and ΔE is the activation energy. The K values were determined by the following expression:

$$K = \frac{P - P_0}{P_0} \times 100 \qquad (7)$$

where P is the parameter value at temperature T and P_0 is the parameter value at room temperature (25°C).

The results obtained for both fibers are shown in Figures 12–17 and the activation energies were calculated from the slopes of the linearity regions and the results are shown in Tables I and II for the Nylon 6 and 6.6 fibers, respectively. Figures 12–17 reveal clearly two kinds of behavior that depend on the analyzed parameter for both fibers.

All the parameters presented two regions of linearity: one at a lower range of temperatures (below the T_g) and another at a higher range of temperatures. The major differences concern the discontinuity regions only. The parameters' shrinkage, LP, and CSs presented discontinuities by a simple change in the slopes of the straight-line regions, while the parameters, $\%C$, and ICP presented a wide range of discontinuity, where the calculated points in this region seem not to fit in any straight line.

The similarities observed for the studied fibers (Nylon 6 and 6.6) are restricted to the existence of such linearity regions as described above. The differences in the crystallization mechanisms are clearly visualized in the activation energies calculated from these straight lines (Tables I and II).

Also, Tables I and II did not reveal any profound differences between the activation energies calculated for both types of annealing conditions (RC and SC). Thus, this result confirms once again the previous discussion where the recrystallization mechanisms presented are very similar for both annealing conditions for both fibers. Actually, only very slight differences in behavior were detected, simplifying here our discussion.

The activation energies for the crystallinity parameter were not calculated due to its poor correlation with the Arrhenius equation, especially in the region between 100 and 170°C. Instead, we

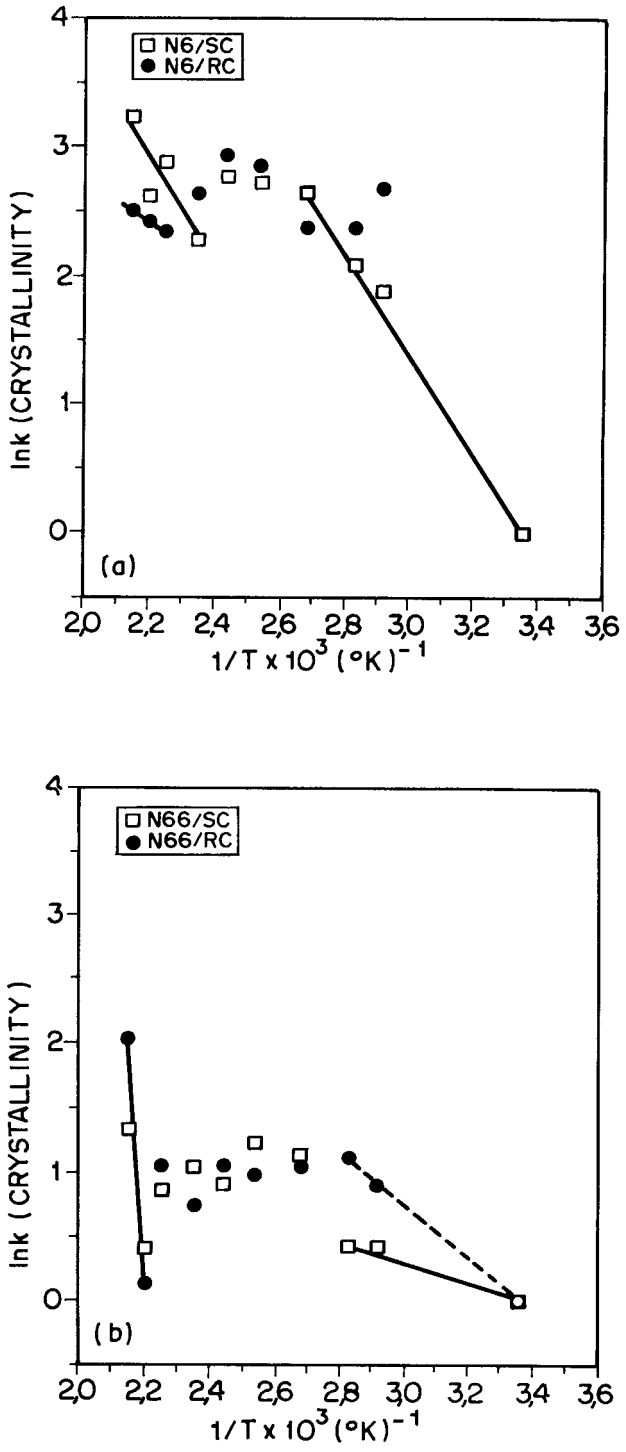

Figure 12 Arrhenius plot for the crystallinity parameter of the (a) Nylon 6 and (b) Nylon 6.6 fibers heat-treated under (□) SC and (●) RC.

preferred to present the activation energies for the ICP parameter whose data obtained from X-ray scattering seems more representative of the chain segment organization within the crystalline regions. An increase in the ICP upon annealing could be a result of small lateral readjustments in interchain positions within a lamella.[1]

The poor correlation of the crystallinity param-

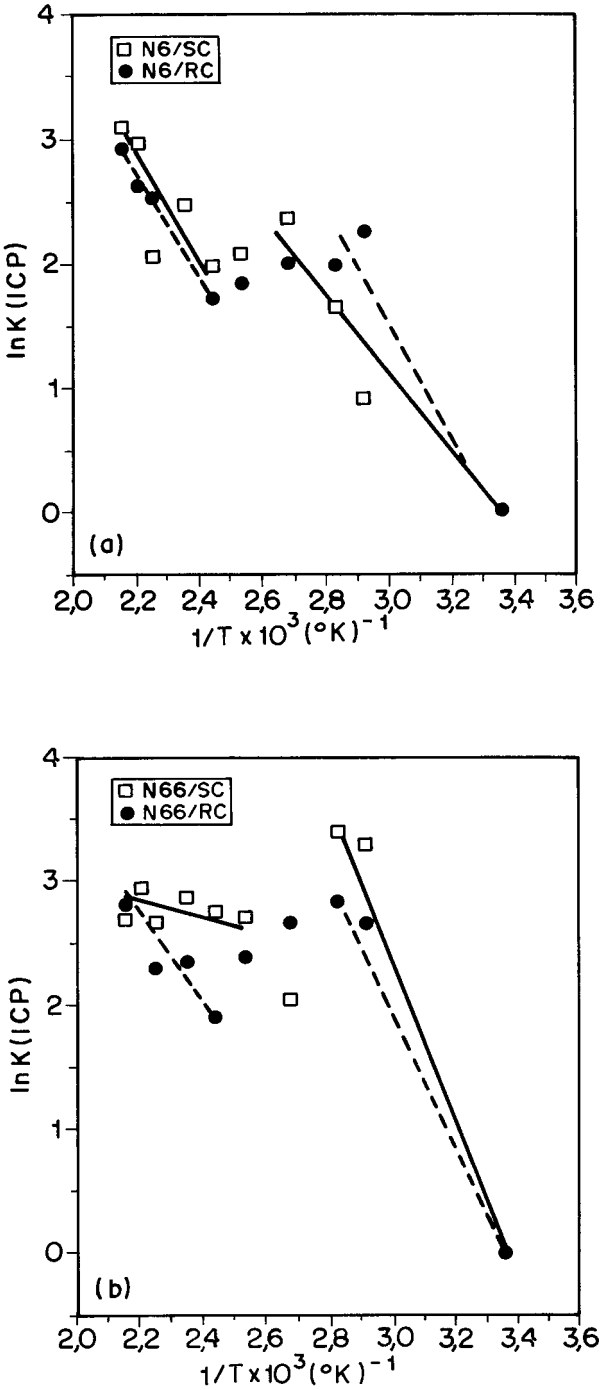

Figure 13 Arrhenius plot for the ICP parameter of the (a) Nylon 6 and (b) Nylon 6.6 fibers heat-treated under (□) SC and (●) RC.

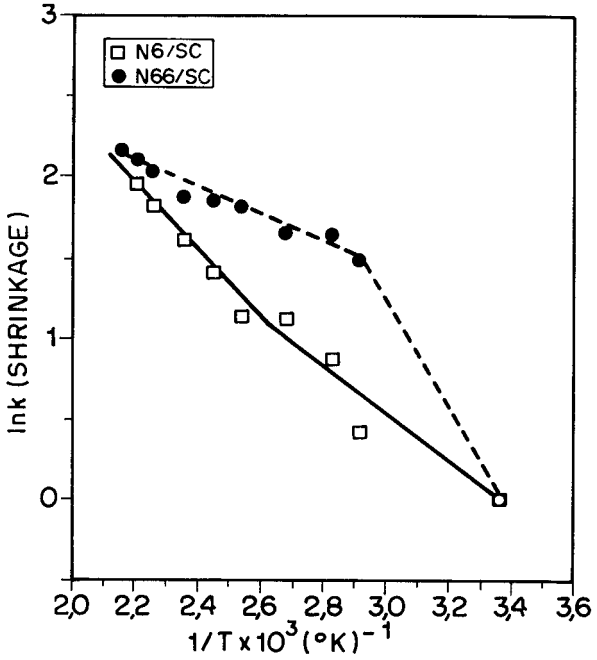

Figure 14 Arrhenius plot for the shrinkage parameter of the (□) Nylon 6 and (●) Nylon 6.6 fibers heat-treated under SC.

eter for these oriented fibers with the Arrhenius equation could be a result of its complex dependence upon several factors such as the extent of orientation of the amorphous and crystalline regions, size and perfection of the crystallites, and how the annealing condition and temperature would affect such factors as mentioned earlier in the text. It is evident from the previous discussion that the disorientation process plays a very important role is the observed loss of the $\%C$ in the annealing temperatures above the T_g for both fibers. Actually, this effect was much greater for Nylon 6.6 than for Nylon 6.

Also, the ICP parameter has been shown to be influenced by the disorientation process, but the straight-line regions obtained in the Arrhenius plots seem to be more reliable to calculate the activation energies and also more representative of the molecular rearrangements within the crystallites during the annealings.

It is interesting to note that at the lower range of annealing temperatures the ΔE values for Nylon 6 are much lower (for most parameters) than the calculated ones for the Nylon 6.6 fibers, but at the higher range of temperatures, the opposite happens, that is, while the activation energies for the Nylon 6.6 decreases accentuately, the calculated values for Nylon 6 increases.

As explained in the first part of this series of articles,[12] the shrinkage mechanism of Nylon 6 will be quite different from the shrinkage mechanism of the Nylon 6.6 fibers. The described mechanisms are strongly dependent on the recrystallization processes which are also quite different, as

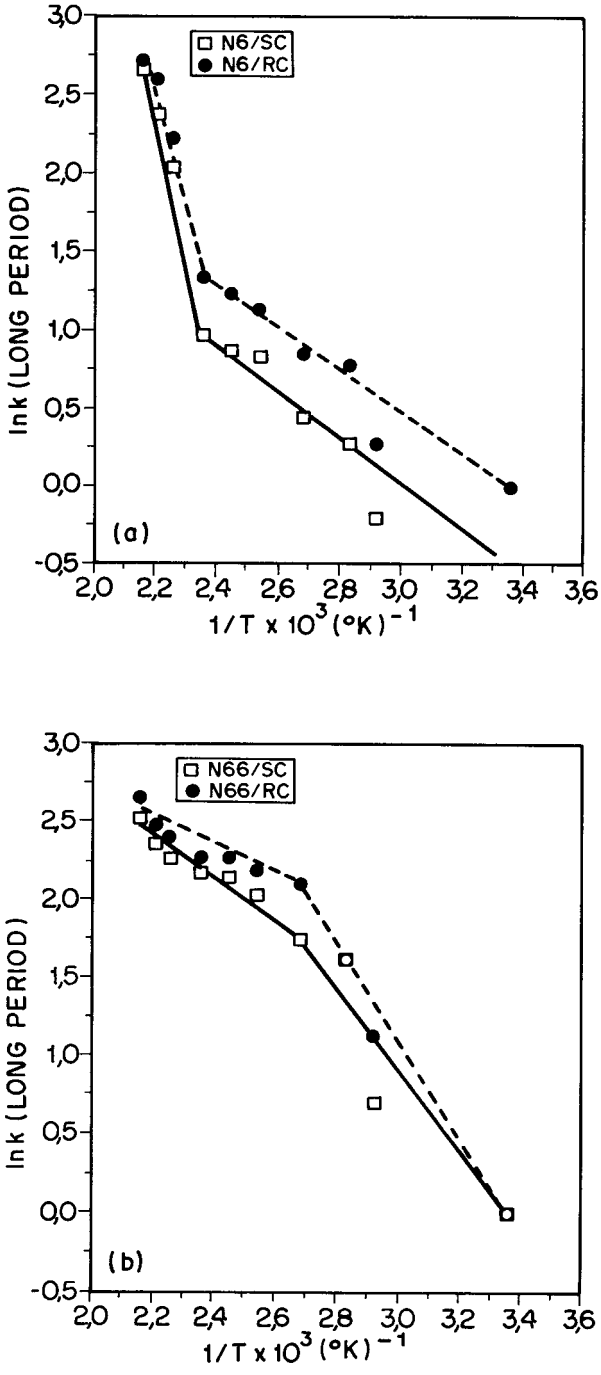

Figure 15 Arrhenius plot for the LP parameter of the (a) Nylon 6 and (b) Nylon 6.6 fibers heat-treated under (□) SC and (●) RC.

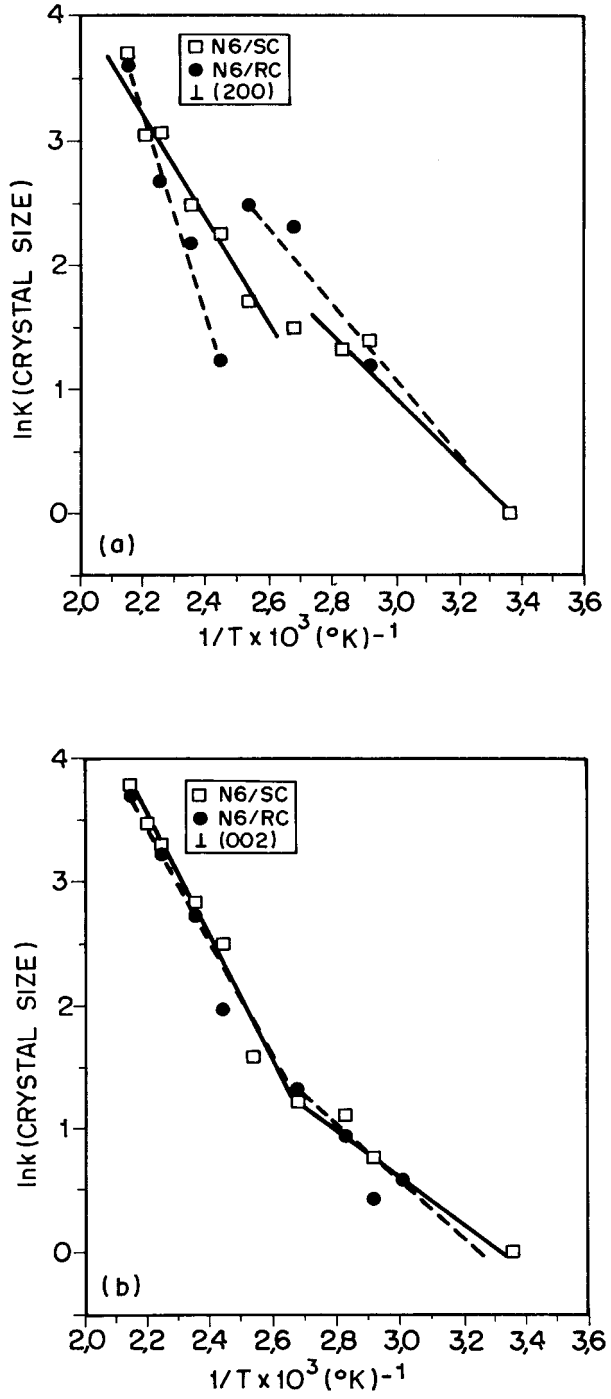

Figure 16 Arrhenius plot for the CS parameter of the Nylon 6 fibers heat-treated under (□) SC and (●) RC: (a) ⊥ (200); (b) ⊥ (002).

shown in this article. While the shrinkage mechanism of Nylon 6 will be difficult by the generation of new tiny crystallites within the interfibrillar regions which will develop at temperatures above 120°C for both types of annealings (RS and SC), the shrinkage mechanism and, consequently, the recrystallization process of Nylon 6.6 will be governed only by the instaneous release and reformation of hydrogen bonds due to the intense chain flexibility that occurs for the annealings above the

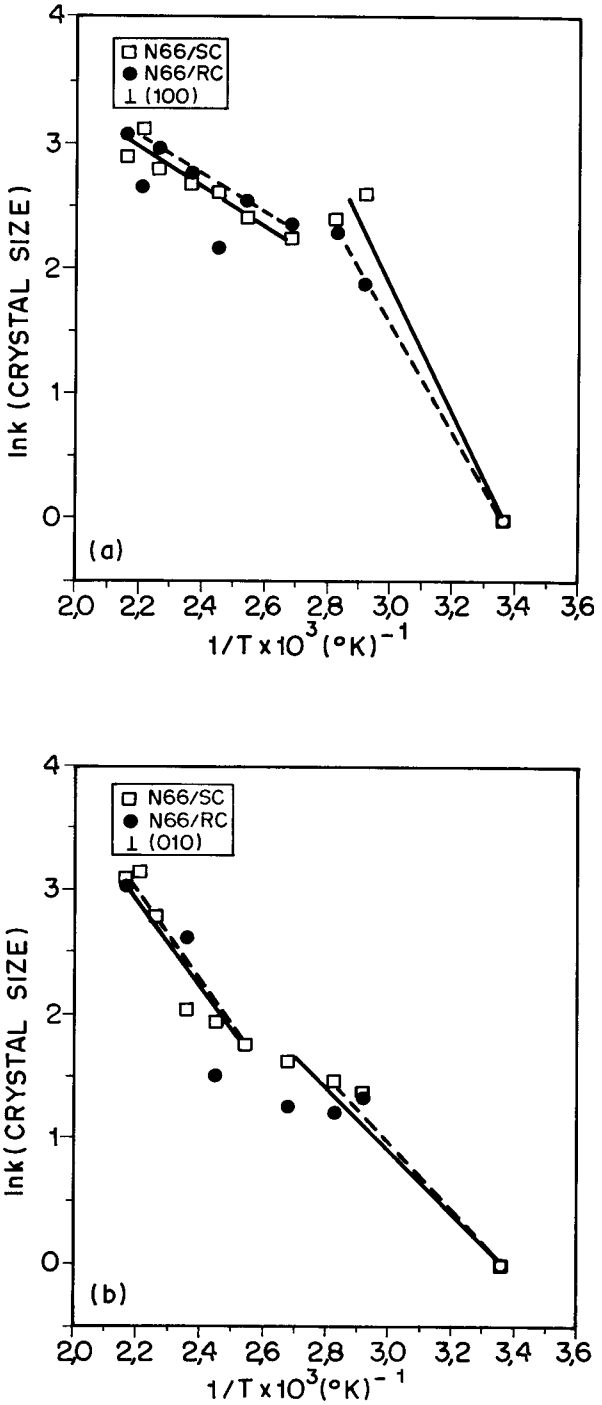

Figure 17 Arrhenius plot for the CS parameter of the Nylon 6.6 fibers heat-treated under (□) SC and (●) RC: (a) ⊥ (100); (b) ⊥ (010).

Table I Activation Energies (ΔE) Calculated from the Tangent of the Straight Lines Observed in the Arrhenius Plots for the Nylon 6 Fibers

Parameter	Type of Heat Treatment	Range of Temperature (°C)	ΔE (cal/mol)
Shrinkage	SC	25–100	3.21
	SC	100–190	5.11
ICP	SC	25–90	6.20
	SC	120–190	7.78
	RC	25–80	8.29
	RC	120–190	8.27
Long period (LP)	SC	25–150	2.30
	SC	150–190	17.22
	RC	25–150	2.81
	RC	150–190	16.89
Crystal size (CS) ⊥ (200)	SC	25–100	4.60
	SC	120–190	9.32
	RC	25–120	6.27
	RC	135–190	15.70
Crystal size (CS) ⊥ (002)	SC	25–100	3.70
	SC	100–190	10.10
	RC	25–100	3.68
	RC	100–190	9.90

T_g of the fiber, with no generation of new crystallites.

So, these different mechanisms are in accordance with the observed differences in the activation energies obtained in the different range of annealing temperatures for both fibers. At annealing temperatures above the T_g of the fibers, the more complex recrystallization process of Nylon 6 with the generation of new crystallites within the interfibrillar regions will require much more energy than will the recrystallization of Nylon 6.6 where only improvement of size and perfection of the preexisting crystals will occur.

At temperatures below the T_g, the Nylon 6.6 fiber will require much more energy to overcome their hydrogen bonds than will Nylon 6. This fact might be the result of the higher structural stability of the Nylon 6.6 fiber as compared to Nylon 6 at room temperature. The inherent structural differences presented by these fibers seem to be responsible for such behavior at lower annealing temperatures.

CONCLUSIONS

The Nylon 6 and 6.6 fibers responded differently to the applied annealings, indicating different recrystallization mechanisms. Although the crystallinity parameter presented three well-defined regions for both fibers at almost the same range of annealing temperatures, the curves were different in format.

The analysis of such curves permitted one to establish the differences in the recrystallization process. In the case of Nylon 6, there was formation of new and very small crystallites in the interfibrillar regions for the annealings performed above 120°C and for both types of heat treatments (SC and RC).

As the annealing temperature increased, there was improvement of size and perfection of such crystallites (by coalescence) and of the preexisting ones. Also, the presence of these new crystallites made difficult the additional loss in the orientation favoring a recrystallization in a preferred direction, that is, in the direction of the fiber axis.

In the case of Nylon 6.6, the DSC thermograms did not reveal formation of such crystallites. So, the disorientation process associated with the release of the hydrogen bonds played a very important role in the recrystallization mechanism of this fiber. Also, the DSC thermograms revealed

Table II Activation Energies (ΔE) Calculated from the Tangent of the Straight Lines Observed in the Arrhenius Plots for the Nylon 6.6 Fibers

Parameter	Type of Heat Treatment	Range of Temperature (°C)	ΔE (cal/mol)
Shrinkage	SC	25–70	6.71
	SC	70–190	1.83
ICP	SC	25–80	13.40
	SC	120–190	0.15
	RC	25–80	11.04
	RC	135–190	6.43
Long period (LP)	SC	25–100	5.07
	SC	100–190	2.24
	RC	25–100	5.13
	RC	100–190	2.10
Crystal size (CS) ⊥ (100)	SC	25–80	9.86
	SC	100–190	2.95
	RC	25–80	8.55
	RC	100–190	2.47
Crystal size (CS) ⊥ (010)	SC	25–100	4.97
	SC	120–190	6.85
	RC	25–80	5.04
	RC	120–190	6.85

two crystallite forms, that is, of the same type but with different degrees of size and perfection. In addition, the changes in the proportion of such crystallite forms with the annealing temperature were very helpful to understand the recrystallization mechanism for the Nylon 6.6 fiber.

At the lower range of temperatures (below the T_g), the defect elimination associated with the global disorientation process prevails, favoring the transformation of less perfect crystallites into more perfect ones. At temperatures above the T_g, a reversal process occurs, that is, the more perfect crystallites are converted again to a more disorganized form. The intense movement of the chain segments would break up their more perfect alignment, establishing a more uniform distribution of the segments although less organized. Finally, the application of the Arrhenius equation to the analyzed structural parameter together with the calculated activation energies for both fibers confirm once more the observed differences.

This research was supported in part by CAPES and in part by FAPESP, which the authors much appreciate. Also, the authors would like to express their gratitude to Dr. Yvonne P. Mascarenhas and the technicians of the Intitute of Physics of São Carlos-USP for permitting and helping the authors with the utilization of their X-ray equipment. We also appreciate the excellent digitation work by Oceania M. Carocci Crnkovic.

REFERENCES

1. N. S. Murthy, H. Minor, and R. A. Latif, *J. Macromol. Sci.-Phys. B,* **26,** 427 (1987).
2. L. A. G. Oriani and A. L. Simal, *J. Appl. Polym. Sci.,* **46,** 1973 (1992).
3. N. S. Murthy, A. C. Reimschuessel, and V. Kramer, *J. Appl. Polym. Sci.,* **40,** 249 (1990).
4. H. A. Kristov and J. M. Schultz, *J. Polym. Sci. Part B Polym. Phys.,* **28,** 1647 (1990).
5. Y. P. Khanna, *J. Appl. Polym. Sci.,* **40,** 569 (1990).
6. D. R. Salem, R. A. F. Moore, and H. D. Weigmann, *J. Polym. Sci. B,* **25,** 567 (1987).
7. H. M. Heuel and R. Huisman, *J. Appl. Polym. Sci.,* **26,** 713 (1981).
8. B. Babatope and D. H. Isaac, *Polymer,* **33,** 1665 (1992).
9. J. W. S. Hearle, *J. Appl. Polym. Sci. Appl. Polym. Symp.,* **31,** 137 (1977).
10. D. C. Prevorsek and H. J. Oswald, in *Solid State Behavior of Linear Polyesters and Polyamides,*

J. M. Schultz and S. Fakirov, Eds., Prentice-Hall, Englewood Cliffs, NJ, 1990.
11. H. J. Oswald, E. A. Turi, P. J. Harget, and Y. P. Khanna, *J. Macromol. Sci. Phys. B,* **13,** 231 (1977).
12. A. L. Simal and A. R. Martin, submitted.
13. G. E. Sweet and J. P. Bell, *J. Polym. Sci. A-2,* **10,** 1273 (1972).
14. M. S. de Araujo and A. L. Simal, *J. Appl. Polym. Sci.,* **60,** 2437 (1996).
15. G. Groeninckx, H. Reynaers, H. Berghmans, and G. Smets, *J. Polym. Sci. Polym. Phys. Ed.,* **18,** 1311 (1980).
16. G. Groeninckx, and H. Reynaers, *J. Polym. Sci. Polym. Phys. Ed.,* **18,** 1325 (1980).
17. I. M. Fouda, M. M. El-Tonsy, and A. M. Shaban, *J. Mater. Sci.,* **26,** 5085 (1991).
18. M. Hirami, *J. Macromol. Sci.-Phys. B,* **23**(4,5), 347 414 (1984–1985).
19. H. W. Starkweather, Jr., P. Zoller, and G. A. Jones, *J. Polym. Sci. Phys.,* **22,** 1615 (1984).
20. P. F. Dismore and W. O. Statton, *J. Polym. Sci. Part C.,* **13,** 133 (1966).
21. L. E. Alexander, *X-ray Diffraction Methods in Polymer Science,* Wiley-Interscience, New York, 1969.
22. D. R. Subramanian, A. Venkataraman, and N. V. Bhat, *J. Macromol. Sci. B,* **18,** 177 (1980).
23. J. H. Dumbleton, D. R. Buchnran, and B. B. Bowles, *J. Appl. Polym. Sci.,* **12,** 2067 (1968).
24. N. V. Bhat and S. G. Naik, *Text. Res. J.,* **54,** 868 (1984).
25. H. W. Starkweather, Jr., *Macromolecules,* **22,** 2000 (1989).
26. J. P. Bell, *Text. Res. J.,* **42,** 292 (1972).